Supporting Information

Atomic-scale imaging of the ferrimagnetic/diamagnetic interface in Au-Fe_3O_4 nanodimers and correlated exchange-bias origin

Liu Zhu[1†], Xia Deng[2†], Yang Hu[1], Jian Liu[3], Hongbin Ma[4], Junli Zhang[1,5], Jiecai Fu[1], Suisui He[3], Jun Wang[1], Baodui Wang[3], Desheng Xue[1] and Yong Peng[1*]

[1]Key Laboratory of Magnetism and Magnetic Materials of the Ministry of Education, School of Physical Science and Technology and Electron Microscopy Centre of Lanzhou University, Lanzhou University, Lanzhou 730000, P. R. China.

[2]School of Life Science and Electron Microscopy Centre of Lanzhou University, Lanzhou University, Lanzhou 730000, P. R. China.

[3]State Key Laboratory of Applied Organic Chemistry and Key Laboratory of Nonferrous Metal Chemistry and Resources Utilization of Gansu Province, Lanzhou University, Lanzhou 730000, P. R. China.

[4]Qinghai Provincial Key Laboratory of New Light Alloys, Qinghai Provincial Engineering Research Center of High Performance Light Metal Alloys and Forming, Qinghai University, Xining 810016, P. R. China.

[5]Division of Physical Science and Engineering, King Abdullah University of Science and Technology (KAUST), Thuwal 239955, Kingdom of Saudi Arabia.

*Corresponding authors

Key Laboratory of Magnetism and Magnetic Materials of the Ministry of Education, Lanzhou University, Lanzhou 730000, P. R. China

E-mail: pengy@lzu.edu.cn (Yong Peng)

†These authors contributed equally to this work.

The diameter statistics and crystal structure of the dumbbell-like Au/Fe_3O_4 nanodimers.

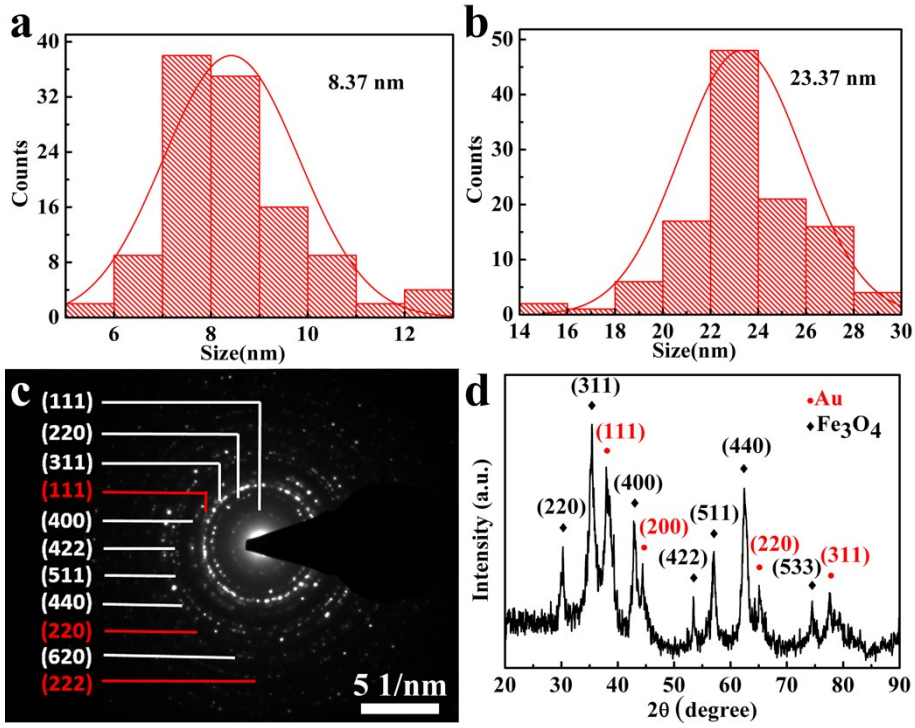

Figure S1. Statistical analysis of the average diameters of Au and Fe_3O_4 components in the dumbbell-like Au-Fe_3O_4 nanoparticles. (a) The average diameter of Au components, ~ 8.4 nm. (b) Average diameter of Fe_3O_4 components, ~ 23.4 nm. (c) and (d) Representative SAED pattern and XRD spectrum detected from a large number of the Au-Fe_3O_4 nanodimers, respectively, indicating that the components of both Au and Fe_3O_4 nanoparticles have a fcc structure.

Figure S1c shows a typical selected-area diffraction pattern (SAED) acquired from a large number of Au-Fe_3O_4 nanodimers. These diffraction rings can be indexed into two sets of lattice planes, including a Au fcc structure with (111), (220) and (222) planes (red marks), and a Fe_3O_4 spinel structure with (111), (220), (311), (400), (422), (511), (440) and (620) planes (white marks). Figure S1d shows a typical X-ray spectrum, revealing the existence of two crystal phases of Au fcc structure and Fe_3O_4 spinel structure. Both SAED and X-ray results are well matched with each other.

Morphological and chemical characterization of Au-Fe_3O_4 nanodimers.

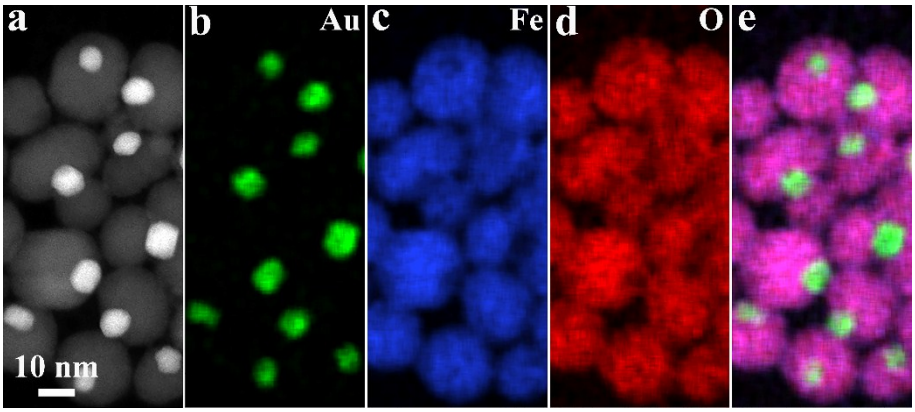

Figure S2. Morphological and chemical characterization. (a) HAADF-STEM image of Au-Fe_3O_4 nanodimers used for EDX elemental mapping analysis. (b-d) Gold, iron and oxygen mapping images. (e) Combined elemental mapping image.

Interface characterization

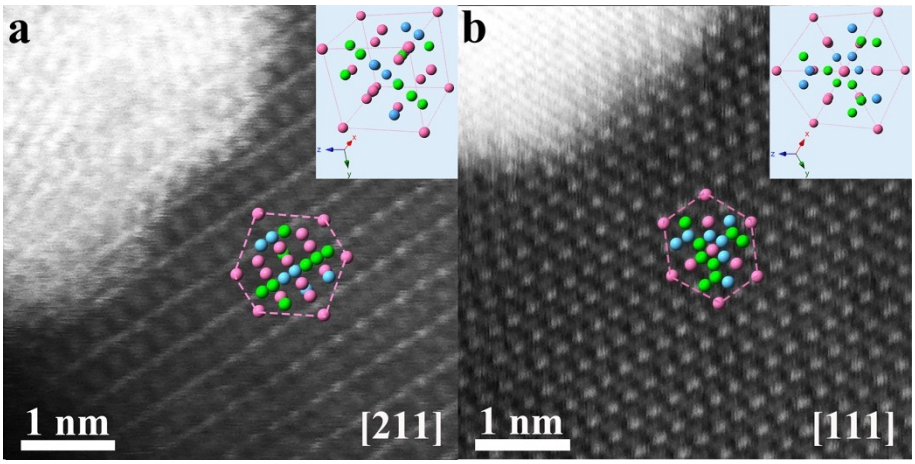

Figure S3. Interface characterization of the Au-Fe_3O_4 nanodimers. (a) and (b) The experimental HAADF-STEM images of the interface of two Au-Fe_3O_4 nanodimers observed along [211] and [111] orientations, respectively, illustrating the growth of Fe_3O_4 component along a particular surface of Au seed. Right-top insets illustrate perspective views of Fe_3O_4 unit-cell models with spinel structure oriented along [211] and [111] orientations, explicitly indicating the distribution of Fe atoms.

Quantitative calculations of the average iron oxidation states of atomic columns across the interface

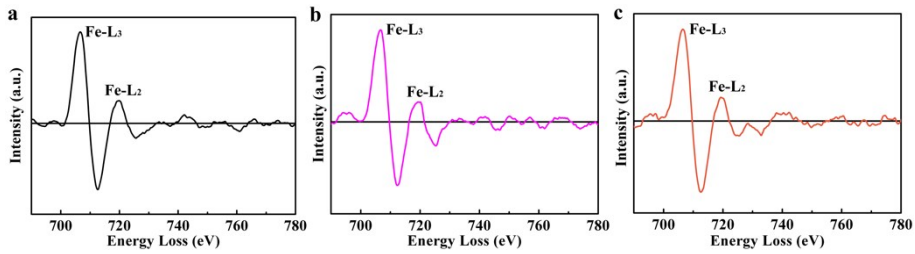

Figure S4. Fe valence state assignments by calculating the intensity ratio of L_3/L_2 in EELS data. (a-c) The corresponding first-derivative EELS spectra of atomic columns 1, 5 and 6 of iron cations after the background subtraction, respectively. Integral intensity ratio between L_3 and L_2 differential peaks is employed to quantify the Fe valence states. The Fe valence states are estimated to be +2.5, +2.35 and +2.43 for the atomic columns 1, 5 and 6, respectively.

The presence of Au atoms replaced the Fe atoms on interfaces in Au-Fe_3O_4 nanodimers accompany a change in the oxidation states of the nearest-neighbor Fe cations as proved in Figure 3b. All of spectra acquired by EELS including Figure 3b have been calibrated on an energy scale by zero-loss peak and deconvoluted by low-loss region to reduce multiple-scattering effect. It is known that in EELS the L edge can provide us with the ionization status of metal cations, of which L_3 and L_2 lines disclose the transitions from $2p^{3/2}$ to $3d^{3/2}3d^{5/2}$ and from $2p^{1/2}$ to $3d^{3/2}$, respectively, and their intensities are related to unoccupied states in the 3d bands. In this work, we used the white line intensity ratio in which background was subtracted by using a power law. Although the reported literatures exist more or less disagreements in the calculation of the normalized white line intensity due to the complexity of EELS theory behind white line and its continuous background, our experience show that the ratio of the white line intensities is more reliable and sensitive. We firstly carried out the first-derivative of the background-subtracted EELS spectra for removing the error of noise and then integrated the L_3 and L_2 differential peaks for the ratio calculations. The 4.35, 4.21 and 4.29 values of peak intensity ratios of Fe L_3/L_2 are calculated for the column 1, 5 and 6, respectively. By comparing with the reference spectra, the Fe valence state in the atomic column 1 is determined to be +2.5, and these of atomic columns 5 and 6 are deduced to be +2.35 and +2.43, which is consistent with the energy shifts of the absorption edges. These results provide clear evidence for the Fe valence state modulation at the interface. Moreover, the Fe valence state is directly

linked with its strength of magnetic moment. The valence changes of interfacial atomic columns 5 and 6 directly prove the existence of magnetic phase transition occurred in the interfaces of the Au-Fe_3O_4 nanodimers.

The calculation of interface spins

Under the consideration as described in the main text which the Fe^{2+} cation in the atomic column 4 of B sites is replaced by a Au atom, each interfacial unit cell will contain six tetrahedral positions occupied by Fe^{3+} cation, six octahedral positions occupied by Fe^{2+} cation, eight octahedral positions occupied by Fe^{3+} cation. Therefore, according the antiferromagnetic and ferromagnetic interactions illustrated by Figure 5b, the average number of spins per interfacial chemical formula can be calculated as following:

$$S_{\mathrm{AFM}} = \frac{8Fe^{2+}B - 2Fe^{3+}A - 2Fe^{2+}B}{8 \times 2} = 1.82$$

The normal unit cell in the body of Fe_3O_4 component remains the normal antiferromagnetic and ferromagnetic interactions of a spinel structure, which have a 3.72 μ_B net moment treated as ferromagnetic layer.[1] Therefore, the average number of spins per chemical formula is 1.86, equal to $S_{FM} = \frac{\mu}{2}$.

As determined by the morphological characterization, the interface diameter is equal to the diameter of Au component. Therefore, the interface area $A_{\mathrm{interface}}$ is 5539Å^2, which can further obtain the per total number of magnetic ions at the interface:

$$N = 24 \times \frac{A_{\mathrm{interface}}}{a^2} = 1896$$

Thus, the number of spin interaction bonds across the interface can be calculated:

$$n_{\mathrm{interface}} = \frac{1}{\sqrt{N}} = 2.3 \times 10^{-2}$$

The calculation of surface spins

For the case of surface disordered layer, the surface area is 42983Å^2. The per total number of magnetic ions at the surface is

$$N = 24 \times \frac{A_{\mathrm{surface}}}{a^2} = 14634$$

Then, the number of spin interaction bonds across the surface can be obtained:

$$n_{\text{surface}} = \frac{1}{\sqrt{N}} = 8.3 \times 10^{-3}$$

Theoretical calculations of exchange bias shift H_{EB} under another two cases: case 1

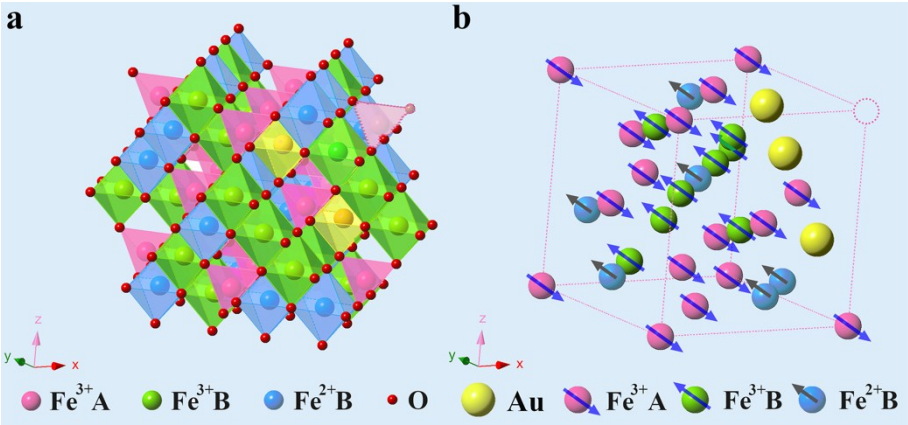

Figure S5. Interfacial occupation and magnetic coupling models. (a) Polyhedral model depicting a face-centered cubic network of red O anions with Fe^{3+} cations labeled as rose red spheres occupying tetrahedral A sites, Fe^{2+} and Fe^{3+} cations occupying octahedral B sites marked by blue and green, respectively. Au atoms taking the place of Fe cations occupying tetrahedral A sites and octahedral B sites are marked as gold spheres, and the dash tetrahedral represents the missing site. (b) The corresponding magnetic coupling model, in which blue arrows represent the magnetic moments (including strength and direction) of Fe^{3+} cations and dark blue arrows represent these of Fe^{2+} cations. The dash sphere represents the missing atom.

When the Fe^{3+} cation in the atomic column 4 of B sites is replaced by a Au atom, the interfacial occupation and magnetic coupling models will become into Figure S5. Therefore, each interfacial unit cell contains 6 tetrahedral positions occupied by Fe^{3+} cation, seven octahedral positions occupied by Fe^{2+} cation, seven octahedral positions occupied by Fe^{3+} cation. Therefore, according the antiferromagnetic and ferromagnetic interactions illustrated by Figure S5b, the average number of spins per interfacial chemical formula S_{AFM} can be calculated to be 1.79. According to the equation 1 in the main text, the exchange bias shift $H_{\text{EB-interface}}$ in this case can be calculated to be 64 Oe.

Theoretical calculations of exchange bias shift H_{EB} under another two cases: case 2

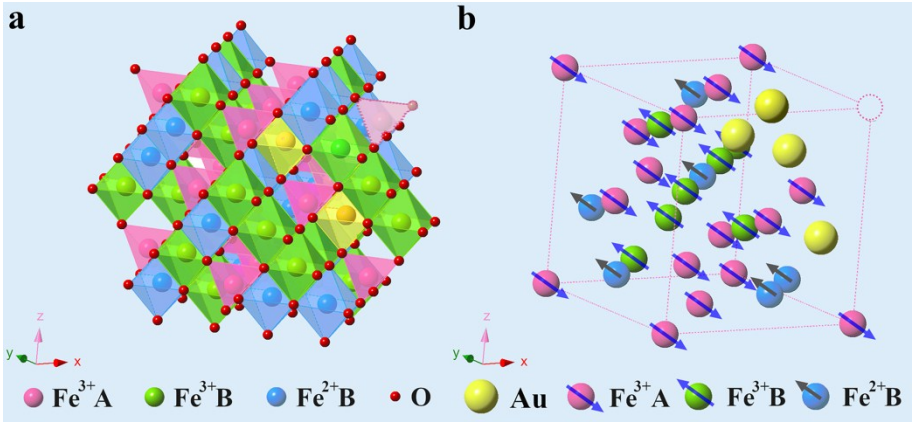

Figure S6. Interfacial occupation models. (a) Polyhedral model depicting a face-centered cubic network of red O anions with Fe^{3+} cations labeled as rose red spheres occupying tetrahedral A sites, Fe^{2+} and Fe^{3+} cations occupying octahedral B sites marked by blue and green, respectively. Au atoms taking the place of Fe cations occupying tetrahedral A sites and octahedral B sites are marked as gold spheres, and the dash tetrahedral represents the missing site. (b) The corresponding magnetic coupling model, in which blue arrows represent the magnetic moments (including strength and direction) of Fe^{3+} cations and dark blue arrows represent these of Fe^{2+} cations. The dash sphere represents the missing atom.

When both Fe^{2+} and Fe^{3+} ions in the atomic column 4 of B sites are replaced by two Au atoms, the interfacial occupation and magnetic coupling models become into Figure S6. Each interfacial unit cell contains 6 tetrahedral positions occupied by Fe^{3+} cation, six octahedral positions occupied by Fe^{2+} cation, seven octahedral positions occupied by Fe^{3+} cation. Therefore, according to the antiferromagnetic and ferromagnetic interactions in Figure S6b, the average number of spins per interfacial chemical formula S_{AFM} can be calculated to be 1.57. Based on the equation 1 in the main text, the exchange bias shift $H_{EB\text{-}interface}$ in this case can be calculated to be 56 Oe.

The exchange bias shift H_{EB} of S2, S3 and S4

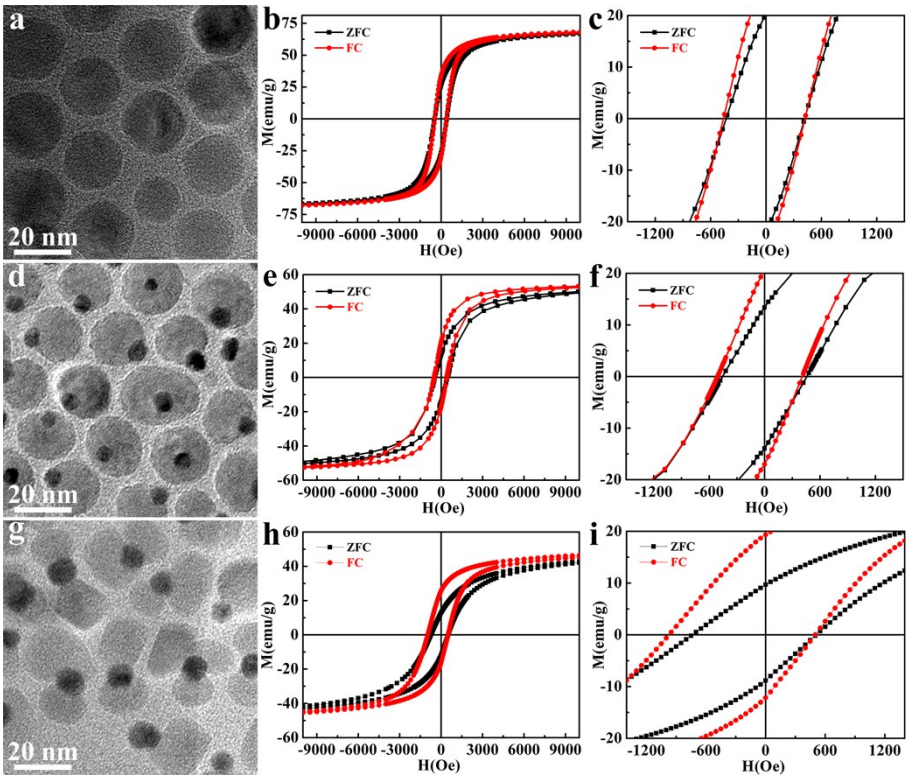

Figure S7. Morphological and magnetic characterization of three compared specimens, including 23 nm pure Fe_3O_4 nanoparticles S2, 5 nm - 23 nm dumbbell-like Au/Fe_3O_4 nanodimers S3, and 8 nm - 23 nm Au-Fe_3O_4 nanoclusters S4. Representative TEM images of (a) S2, (d) S3 and (g) S4. Magnetization hysteresis loops of (b) S2, (e) S3 and (h) S4 measured at 2 K. The center enlarged views of the ZFC and 5T-FC field-dependent-magnetization curves for (c) S2, (f) S3 and (i) S4.

In order to confirm the observed EB mechanism of interface interactions of weak/strong ferrimagnetic bilayer in the ferrimagnetic/diamagnetic coupled Au-Fe_3O_4 nanodimers, we performed a series of compared experiments. Another three types of specimens were fabricated to make comparisons, including 23 nm pure Fe_3O_4 nanoparticles (specimen S2), 5 nm-23 nm dumbbell-like Au-Fe_3O_4 nanodimers with smaller Au components (specimen S3) and 8 nm-23 nm Au-Fe_3O_4 nanoclusters (specimen S4) as shown in Figure S7a, S7d and S7g. Their relevant field dependence of magnetization loops are shown in Figure S7b, S7e and S7h, whose center enlarged views are shown in Fig. S7c, S7f and S7i. The FC loops show a 19 Oe exchange bias value of S2, 51 Oe HEB of S3 and 237 Oe HEB of S4. Theoretical exchange bias shift H_{EB} of S2 can be calculated to be 24 Oe, matching with its 19 Oe experimental data. This agreement further verifies that the disordered surface moments of Fe_3O_4

components contribute a small part of exchange bias shift. In the case of S3, the average interface size is almost equal to the diameter of Au components. Therefore, the interface area $A_{\text{interface - S3}}$ is approximately equal to $0.35A_{\text{interface - S1}}$, which can further obtain the exchange bias shift $H_{\text{EB-interface}}$ of S3:

$$H_{\text{EB-interface-S3}} = 0.35\ H_{\text{EB-interface-S1}} = 23\ \text{Oe}$$

A 23 Oe $H_{\text{EB-interface}}$ coming from the interface of the S3 is then theoretically calculated. Considering disordered surface moments, a 24 Oe of surface exchange bias ($H_{\text{EB-surface}}$) can be calculated. Therefore, a total of 47 Oe exchange bias shift $H_{\text{EB-total}}$ can be theoretically obtained, which is very close to the above experimental value of 51 Oe. As the diameter of Au components in this S3 specimen is smaller than that of S1 in the main text, both decreased EB values of experimental measurement and theoretical calculation are well fitted with the predicated trend. For the case of S4, it possesses the bigger interfacial area between the Au and Fe_3O_4 components than that of S1 and S3. According to the TEM image shown in Fig. S7g, 2.2 times interface area can be estimated in comparison with S1. Therefore, the exchange bias shift of S4 can be calculated as following:

$$H_{\text{EB-mixture}} = 2.2\ H_{\text{EB-dimer}} = 206\ \text{Oe}$$

This value is close to the measured value of 237 Oe. From these comparisons, it further proves that the interface interaction of weak/strong ferrimagnetic bilayer in ferrimagnetic/diamagnetic coupled Au-Fe_3O_4 nanodimers is mainly responsible to the origin of their EB effect.

In addition, the coercivities (H_c) of the S2, S3 and S4 are 440 Oe, 458 Oe and 736 Oe, respectively, which imply a population of both pinned and unpinned uncompensated spins at the interface. Pinned uncompensated spins remain anchored to the antiferromagnet upon cycling the magnetic field and induce H_E, as observed from the shifted hysteresis loop in Figure S7. Unpinned uncompensated spins rotate with the ferrimagnet, through a spin drag effect and result in the enhanced coercive field.

Theoretical calculations of saturation magnetization and coercivity

When the magnetic properties of Au-Fe_3O_4 nanodimers were measured, organics covered on the surfaces of specimens were not washed. In order to accurately calculate the intrinsic saturation magnetization (*Ms*), inductively coupled plasma

method to measure the concentrations of gold ions and iron ions. Supplementary table 1 shows the corresponding data. According to the concentration of iron ions, it is calculated that the percentage of Fe_3O_4 component is 60.34%. Furthermore, on the basis of the ratio of Fe_3O_4 among the total weight of the specimen, a 51.43 emu/g *Ms* value of our Au-Fe_3O_4 nanodimers can be calculated. This value is very close to the experimentally measured value of 49 emu/g at 2 K shown in Figure 4b, revealing a good match with the experimentally structural characterization.

Table S1. Elemental concentration percentage measured by inductively coupled plasma

Element	Au	Fe
Percentage (%)	9.74	43.70

We also analyse the coercivity of the Au-Fe_3O_4 nanodimers. It was measured that the diameter of Fe_3O_4 components is 23.4 nm, which is smaller than the critical diameter of single domain for Fe_3O_4. Equation $H_C = \frac{2K1}{\mu 0 M_S}$ is then employed to theoretically analyse the coercivity of the Au-Fe_3O_4 nanodimers, which gives a 411 Oe value. This value is nearly the same as the value (460 Oe) we measured experimentally. Both magnetic parameters well matching with their morphological and structural observation of STEM images verify our finding that the exchange-bias origin of the ferromagnetic/diamagnetic coupled Au-Fe_3O_4 nanodimers originates from magnetic phase transition from another perspective.

References

1. Antonov, V. N.; Harmon, B. N.; Yaresko, A. N., Electronic structure and x-ray magnetic circular dichroism in Fe_3O_4 and Mn-, Co-, or Ni-substituted Fe_3O_4. *Phys. Rev. B* **2003,** *67*, 024417.